V. G. Kiptily, J. M. Adams, L. Bertalot, A. Murari, S.E. Sharapov, V. Yavorskij,
B. Alper, R. Barnsley, P. de Vries, C. Gowers, L.-G. Eriksson, P.J. Lomas,
M. J. Mantsinen, A. Meigs, J.-M. Noterdaeme, F.P. Orsitto
and JET EFDA contributors

Gamma-Ray Imaging of D and ^{4}He Ions Accelerated by Ion-Cyclotron-Resonance Heating in JET Plasmas

Gamma-Ray Imaging of D and ^{4}He Ions Accelerated by Ion-Cyclotron-Resonance Heating in JET Plasmas

V. G. Kiptily[1], J. M. Adams[1], L. Bertalot[2], A. Murari[3], S.E. Sharapov[1], V. Yavorskij[4,5], B. Alper[1], R. Barnsley[1], P. de Vries[1], C. Gowers[1], L.-G. Eriksson[6], P.J. Lomas[1], M.J. Mantsinen[7], A. Meigs[1], J.-M. Noterdaeme[8,9], F.P. Orsitto[2] and JET EFDA contributors*

[1]*EURATOM/UKAEA Fusion Association, Culham Science Centre, Abingdon, Oxon, OX14 3DB, UK*
[2]*Ass. EURATOM/ENEA/CNR sulla Fusione, Centro Ricerche Energia ENEA-Frascati 00044, Rome, Italy*
[3]*Consorzio RFX - Associazione Euratom-Enea sulla Fusione, I-35127 Padova, Italy*
[4]*EURATOM/OEAW Association, Institute for Theoretical Physics, University of Innsbruck, Austria*
[5]*Institute for Nuclear Research, Kiev, Ukraine*
[6]*Ass. EURATOM/CEA, CEA/DSM/DRFC, CEA-Cadarache, 13108 St Paul-lez-Durance, France*
[7]*Helsinki University of Technology, Association Euratom-Tekes, P.O.Box 2200, FIN-02015 HUT, Finland*
[8]*Max-Planck IPP-EURATOM Assoziation, Garching, Germany*
[9]*Gent University, Department EESA, Belgium*
* *See annex of J. Pamela et al, "Overview of Recent JET Results and Future Perspectives", Fusion Energy 2002 (Proc. 19th IAEA Fusion Energy Conference, Lyon (2002).*

ABSTRACT.

Gamma-ray images of fast D and ^{4}He ions accelerated with third-harmonic ion-cyclotron resonance heating of ^{4}He-beam were simultaneously recorded for the first time in JET tokamak experiments dedicated to the investigation of burning plasmas with 3.5-MeV fusion alpha (α) particles. Gamma (γ) rays, born as a result of nuclear reactions ^{9}Be(α,n γ) ^{12}C and ^{12}C(d,p γ) ^{13}C between the fast ions and the main plasma impurities, are measured with a 2-D multicollimator spectrometer array, which distinguishes the γ-rays from accelerated D and ^{4}He-ions. Tomographic reconstruction of the γ-ray emission profiles gives images of the fast-ion population in the poloidal cross-section. The potential of this technique to visualise several energetic ion species and to determine their behaviour in different plasma scenarios is demonstrated.

INTRODUCTION

The study of fast ions in tokamak plasma experiments is an important part of today's magnetic fusion programme. It includes development of the Ion Cyclotron Range Frequency (ICRF) heating scenarios, which could provide effective mechanisms for additional heating of reactor plasmas, and investigation of the behaviour of ions in the MeV-energy range to model the heating of the plasma by fusion α-particles. Simultaneous measurements of several fast-ion species are paramount for the burning plasma in ITER. At least two types of fast ions are expected in the ITER plasma: 1MeV deuterons from NBI heating and fusion α particles (^{4}He), which are born in the reaction D+T $\rightarrow$ α (3.5MeV) + n (14MeV). A principal diagnostic problem in ITER will be discriminating the NBI deuterium from the fusion α particles. This Letter shows for the first time that a simultaneous measurement of fast D- and ^{4}He-ions is possible with γ-ray diagnostics.

The γ-ray technique, now routinely used for the fast-ion study in JET [1-4], is based on measurements of γ-rays, which are born as a result of nuclear reactions between fast ions and the main plasma intrinsic impurities in JET (C, Be). This diagnostic provides information on the energetic ion tail and spatial distribution of γ-ray emission.

This Letter reports on the first γ-ray images of D- and ^{4}He-ions obtained with two-dimensional array of collimated γ-ray spectrometers, the so-called Gamma Cameras. The use of the γ-spectrometers has allowed us to essentially increase the efficiency of the measurements, and gave the opportunity to detect γ-rays in the specific adjustable energy windows that are crucial for distinguishing the emissions from different fast ion species in plasmas. Gamma-ray image of fast ^{4}He-ions was recorded during plasma heating with third-harmonic Ion-Cyclotron-Resonance Heating (ICRH) of ^{4}He beam-ions [5] in the experiment, which was dedicated to simulation of burning plasmas with 3.5MeV fusion α particles. Simultaneously, D-minority was accelerated by the same 3rd harmonic ICRH, and also related γ-ray emission profile was measured in different energy range. These measurements provide information on the localisation of energetic D- and ^{4}He-ions in the plasma, and show clear difference in γ-ray images depending on the fast ion orbits in a monotonic and non-monotonic q-profile plasma, providing very important information for the development of reactor plasma scenarios.

In α-particle simulation experiments with third harmonic heating of ^{4}He-beam in ^{4}He-plasmas, γ-radiation due to the nuclear reaction ^{9}Be(α,n γ) ^{12}C was detected, showing the successful ICRF-acceleration of 4He-beam ions as intended. The diagnostic capabilities of the reaction ^{9}Be(α,n γ) ^{12}C are determined by the specific reaction cross-section [3]. The first energy level 4.44MeV of the final nucleus, ^{12}C, is excited by α particles, and as result the peak at 4.44MeV (transition $4.44 \rightarrow 0$) in the spectrum appears. The γ-ray emission from the reaction ^{12}C(d,p γ) ^{13}C was observed as well. A peak at 3.09MeV (transition $3.09 \rightarrow 0$), which is identified as a γ-emission from the ^{12}C(d,p γ) ^{13}C reaction, reflects the presence in the plasma of the fast D-ions in the MeV-range. This evidence indicates that the deuterium minority also absorbs some ICRF power at the third harmonic D resonance that coincides with the third harmonic ^{4}He resonance. Figure 1 shows the γ-ray spectra recorded in two similar discharges with a high-resolution NaI(Tl) spectrometer. It is seen that when the 110keV neutral beam heating injector was replaced by the 70keV one with the same power, the intensity of the 4.44MeV γ-emission fell substantially whereas deuterium γ-peak did not change. This effect can be explained by decreasing single pass ^{4}He damping of the ICRF waves due to the smaller value of the finite Larmor radius that determines the third harmonic absorption. As follows from the γ-ray spectrum analysis with the GAMMOD code [3], the effective tail temperature $<T_{He}>$, which is used as a parameter to describe the distribution function of fast ^{4}He-ions, falls from 0.5MeV to 0.35MeV, while the deuterium tail-temperature $<T_D>$ does not change. In these experiments the reaction-rates $R(E) \propto \sigma(E) \sqrt{E} f(E)$ where $\sigma(E)$ is a nuclear reaction cross-section, $f(E)$ is a fast ion energy distribution function, are presented in Fig.2. One can see the 4.44MeV γ-ray emission from the ^{9}Be (α,n γ) ^{12}C reaction is produced by ^{4}He-ions in the narrow energy band around the energy 2MeV. At the same time, a rather broad band of D-ions (0.8 ÷ 2.5MeV) gives rise to the 3.09MeV gammas due to the reaction ^{12}C(d,p γ) ^{13}C.

Spatial profiles of the γ-ray emission in the energy range Eg>1 MeV have been measured in JET using the Gamma Cameras, which have ten horizontal and nine vertical collimated lines of sight. The detector array is comprised of 19 CsI(Tl) photo-diodes (10mm × 10mm × 15mm). The CsI(Tl) detectors are well calibrated with radioactive sources ^{22}Na (511, 1275 keV), which are embedded in the detector-array module. The data acquisition system accommodates the γ-ray count-rate measurement in four independently adjustable energy windows. This allows allocating γ-ray peaks for a given fast ion population in specific windows to count them separately. The most recent Monte-Carlo calculations of the detector response function show that size of the CsI(Tl) scintillator is suitable for the γ-ray measurements in the MeV-range. It is found that noticeable contribution to the γ-ray spectrum with energy $E_\gamma >> 2m_e c^2$ gives so-called single- and double-escape peaks, which result from the high probability of $e^- e^+$ –pair generation in the detector. The detector efficiency in this case is sufficient for reliable counting.

In the Gamma Cameras the measurable line-integral γ-ray brightness along the viewing direction can be represented in simplified form as

2

$$\Gamma \propto \int_E \sigma(E) \sqrt{E} dE \int_L n_Z(r) \, F(E;r, \theta) dl \qquad (1)$$

where $F(E;r,\theta)$ is a fast-ion distribution function, depending on the ion energy, minor radius and poloidal angle; (r) n Z is a low-Z impurity density. Experimental data obtained for the 19 lines of sight are tomographically reconstructed to get the local gamma-ray emissivity in a poloidal cross-section, $I(r, \theta) \propto n_Z \int_E F(E;r, \theta) \, \sigma(E) \sqrt{E} dE$. In these reconstructions the full geometry of the collimators and detector efficiencies were taken into account, but small effects of attenuation and scattering of the γ-rays were neglected. It is assumed that the distribution of the low-Z impurities is uniform in the plasma core as confirmed by atomic spectroscopy measurements. For the tomographic reconstruction a constrained optimisation method [6] is used, which was successfully applied earlier to soft x-ray, bolometer and γ-ray measurements at JET[3,6]. The effective spatial resolution of the diagnostic is about ±6cm.

The special energy windows, containing the 3.09MeV and 4.44MeV peaks with their single and double escape satellites were set up to measure spatial profiles of the γ-ray emission from D and [4]He-ions. A typical example of the tomographic reconstruction of the measured line-integrated profiles recorded during 1s in a steady state phase of the plasma discharge is shown in Fig.3. It is seen clearly that the γ-ray emission profile produced by fast D-ions (right-hand figure) differs from the profile from [4]He-ions (left-hand figure). This effect can be explained by the difference in pitch-angle distribution between [4]He beam-ions injected into the plasma quasi-tangentially and isotropic D-minority ions. Furthermore, as seen in Fig.2, the D-minority ions, unlike the [4]He-ions, produce γ-rays in the broad band of energies, and so the D-ions with different orbit topologies contribute to the γ-ray emission profile. Figure 4 shows the typical orbits of the ICRF accelerated D and [4]He-ions (with v_{ll} close to zero at resonance layer $R_{res} = 3m$), which mainly contribute to the observed γ-ray emission. They were calculated for the magnetic configuration for this particular discharge. For the D-ions the orbits were calculated in the broad energy range: 1.0, 1.5 and 2.0MeV. For the [4]He-ions the most probable energy value, 1.9MeV, was chosen in accordance with Fig.2.

The ability to separate γ-rays from different energy bands allows the study of the fast ion behaviour in some important plasma scenarios with the Gamma Cameras. For instance, a unique γ-ray emission profile produced by [4]He-ions was measured in an advanced regime plasma discharge. In this discharge Alfvén cascade and reverse-shear sawtooth instabilities were observed indicating a non-monotonic safety factor (q) profile [7]. According to theoretical analysis of fast α-particle orbit topology in non-monotonic q-profile plasmas [8], very broad confined banana orbits are expected for the [4]He-ions with energies around 2MeV. The γ-ray emission profile presented in Fig.5 (left) is consistent with this prediction. Actually, the calculated orbits (typically, with v_{ll} close to zero at the resonance layer $R_{res} = 3m$ and almost a stagnation orbit) of a probe 1.9MeV [4]He-ion in a plasma configuration with deeply reversed magnetic shear (Fig.6) demonstrates that the model with a

moderate current hole size (r<0.3a) corresponds to the measured γ-ray emission profile. It is expected that the ^{4}He-ions with near-stagnation orbits mostly contribute to the γ-ray emission observed in the region R>R_{res}. In the same discharge, in the phase with a monotonic q-profile, a γ-ray emission profile was observed (Fig.5, right), which is consistent with the calculated standard banana-orbit as presented in Fig.4 (left).

It is worth stressing that in a long-term perspective similar measurements with 2-D cameras could be used in the burning-like ITER plasmas, but the γ-ray detectors should be protected against severe neutron emission with special neutron filters [9]. Since the main impurity in ITER plasmas will probably be beryllium, the slowed deuterons will give rise to gammas (2.88MeV and 3.37MeV) from the ^{9}Be(d,n γ) ^{10}B and ^{9}Be(d,p γ) ^{10}Be reactions, whereas the fusion alphas with energies around the 2MeV resonance in the ^{9}Be(α,n γ) ^{12}C reaction produce 4.44MeV gammas. Using γ-ray spectrometers in every channel of the ITER cameras, the α-particle slowing down profile can be measured with the technique successfully tested in JET Trace Tritium Experiments [10]. Simultaneous measurements of the NBI power deposition and α-particle slowing down profiles are very important for the optimisation of different plasma scenarios and understanding of the fast-ion confinement effects for further progress on the way to DT-ignition.

REFERENCES
[1]. Sadler G.J. et al 1990 Fusion Technology **18** 556

[2]. Jarvis O.N. et al 1996 Nucl. Fusion **36** 1513

[3]. Kiptily V.G. et al 2002 Nucl. Fusion **42** 999

[4]. Kiptily V.G. et al 2003 Rev. Sci. Instrum. **74** 1753

[5]. Mantsinen M. et al 2002 Phys. Rev. Lett. **88** 105002

[6]. Ingesson L.C. et al 1998 Nucl. Fusion **38** 1675

[7]. Sharapov S.E. et al 2002 Phys. Plasmas **9** 2027

[8]. Yavorskij V. et al 2003 Nucl. Fusion **43** 1077

[9]. Kiptily V.G. et al 1998 Technical Physics **43** 471

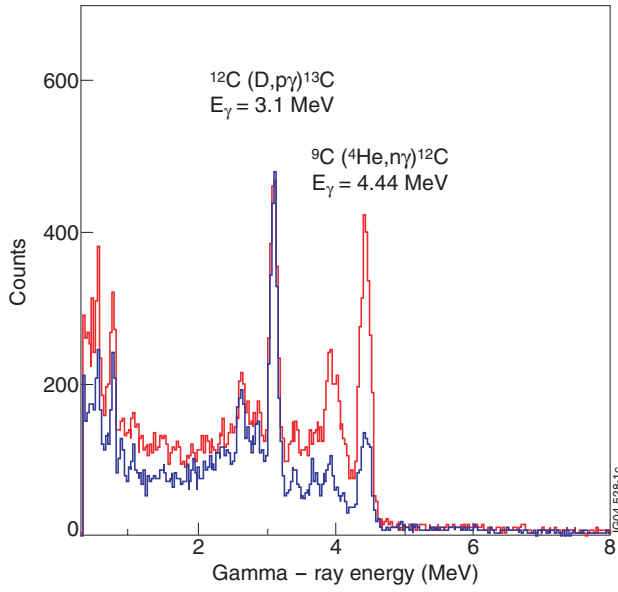[10]. Kiptily V.G. et al 2004 Phys. Rev. Lett. **93** 115001

Figure 1: Gamma-ray spectra measured by the NaI(Tl) detector: red line – spectrum recorded in discharge with 70keV and 110keV ^{4}He-beam injectors; blue line – spectrum recorded in a discharge with two 70keV ^{4}He-beam injectors.
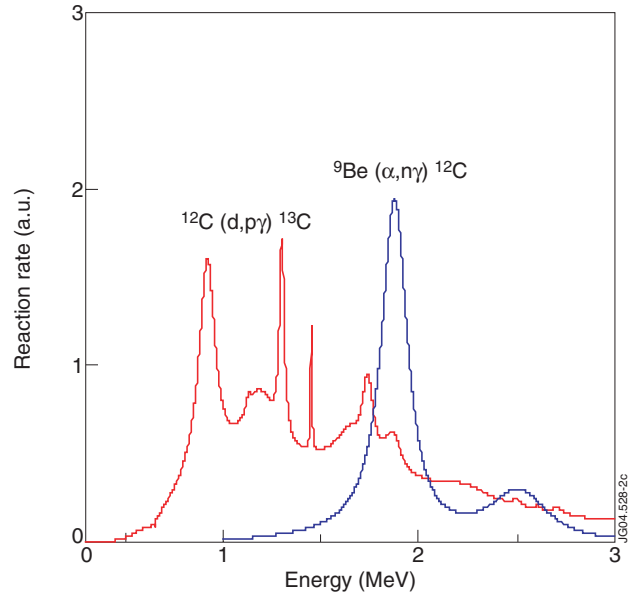

Figure 2: Calculated reaction-rates for the typical distribution functions of D and ^{4}He-ions deduced from γ-ray measurements in these experiments.
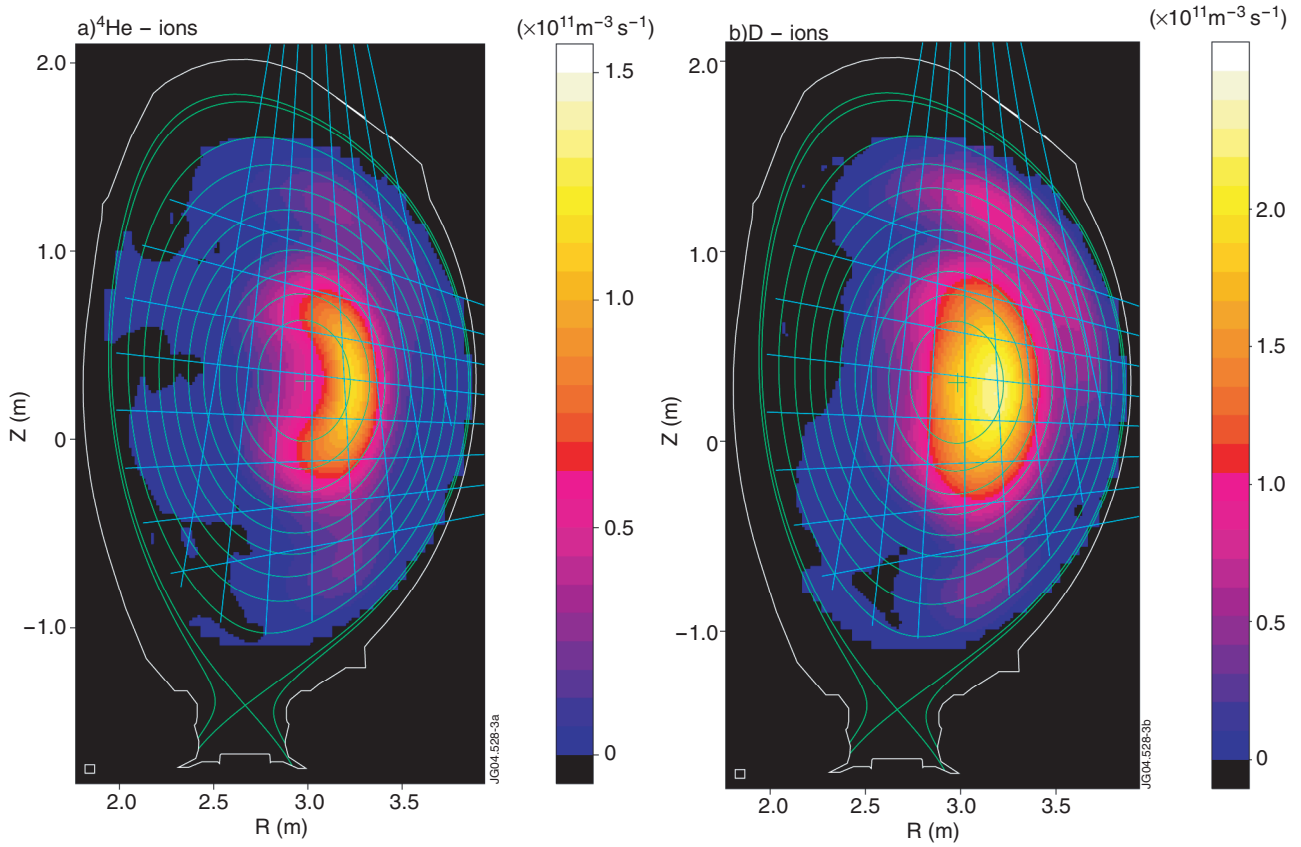

Figure 3: Tomographic reconstructions of 4.44MeV γ-ray emission from the reaction ^{9}Be(α,n γ) ^{12}C (left) and 3.09MeV γ-ray emission from the reaction ^{12}C(d,p γ) ^{13}C (right) deduced from simultaneously measured profiles.
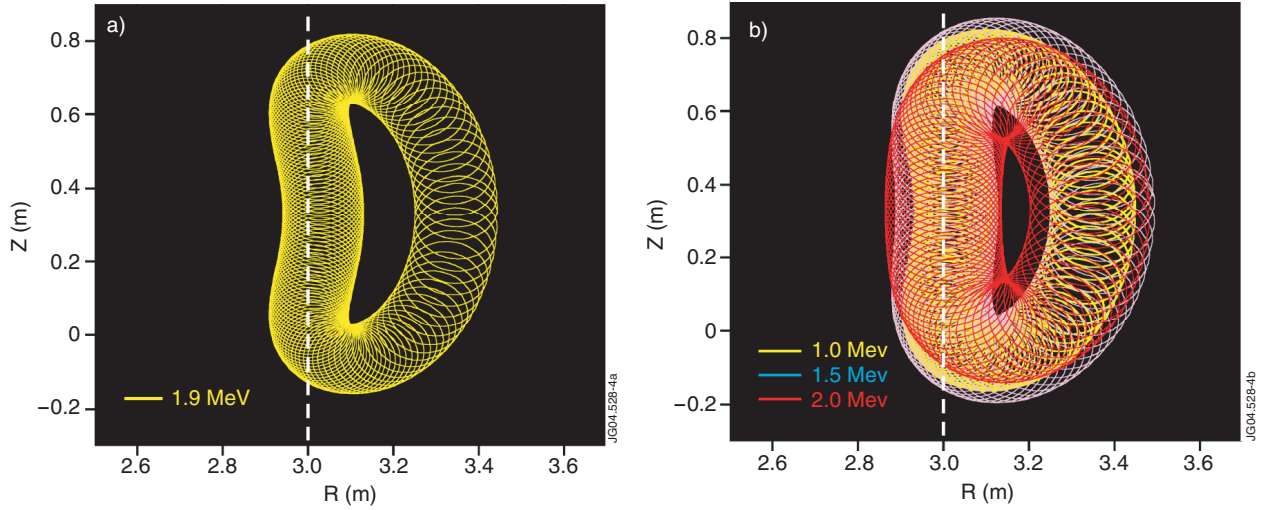
5

Figure 4: Calculated orbits of ^{4}He-ions with energy 1.9MeV (left) and D-ions with energy 1, 1.5 and 2MeV (right) in the same magnetic configuration as in the experiment.
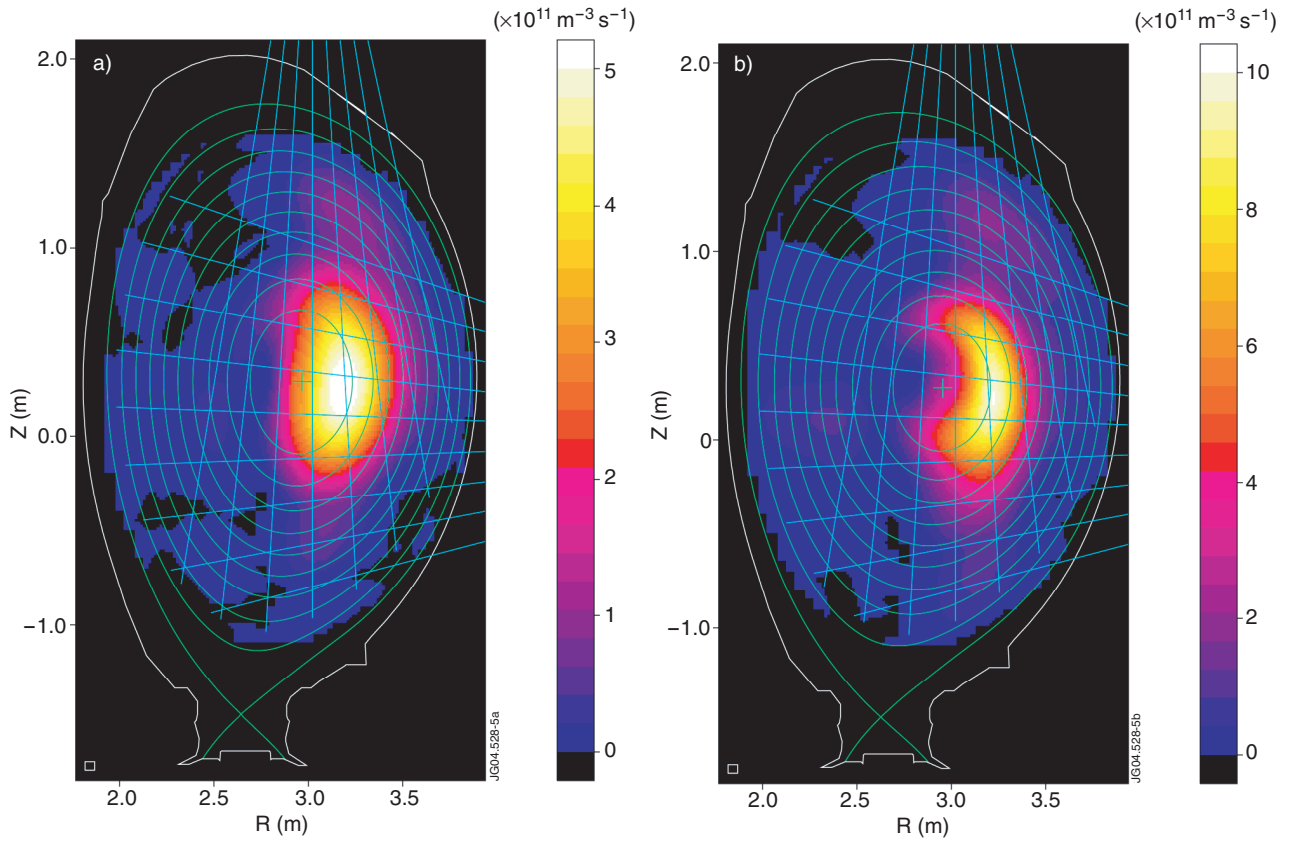

Figure 5: Tomographic reconstructions of the 4.44MeV γ-ray emission from the reaction $^9Be(\alpha,n\ \gamma)\ ^{12}C$ related to profiles measured in the non-monotonic (left) and monotonic (right) q-profile phases of the same plasma discharge
.

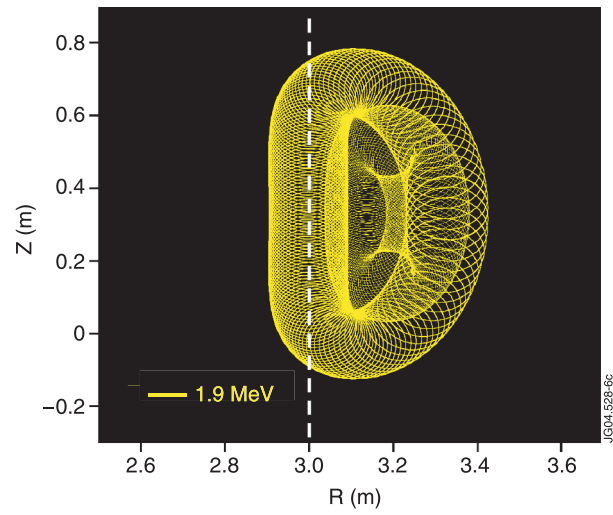*Figure 6: Calculated orbits of the ^{4}He-ion in the discharge with a non-monotonic q-profile.*